

## Three-Dimensional Kinematics of an Unconstrained Ankle Arthroplasty: A Preliminary *In Vivo* Videofluoroscopic Feasibility Study

Renate List, PhD<sup>1</sup>; Mauro Foresti, PhD<sup>1</sup>; Hans Gerber, PhD<sup>1</sup>; Jörg Goldhahn, MD<sup>1</sup>; Pascal Rippstein, MD<sup>2</sup>; Edgar Stüssi, MD<sup>1</sup>  
Zurich, Switzerland

### ABSTRACT

**Background:** Understanding the functionality of total ankle arthroplasties (TAA) requires thorough knowledge of the kinematics during activities of daily life. Videofluoroscopy enables the *in vivo* measurement of the 3D kinematics of implant components more accurately than by means of skin marker tracking. The aim of the present preliminary study was to quantify the 3D kinematics of a TAA during the stance phase of level and slope walking using single plane videofluoroscopy. **Methods:** The experimental set up consisted of a videofluoroscopy system (BV Pulsera, Philips Medical Systems, Switzerland, 25 Hz, 1 ms shutter time) integrated in a walkway, allowing the assessment of free level gait, uphill, downhill and cross-slope walking. 2D/3D registration was performed using the CAD models of the TAA. In a preliminary feasibility study, the presented method was applied on four patients with successful unilateral TAA (Mobility™ Total Ankle, DePuy) with good outcomes. **Results:** Isolated 3D TAA kinematics was quantified with a rotational and translational error of 0.2 degrees and 0.4 mm in plane and 1.3 degrees and 2.1 mm out of plane. In the feasibility study it was found that only minor limitations occurred in sagittal plane motion. Any restrictions were caused by a limitation in dorsiflexion, whereas plantarflexion was for all gait conditions sufficiently provided. Transverse and frontal plane rotation was marginal, the main rotation occurred around the

talar construction axis itself. **Conclusion:** The presented method enabled accurate estimation of the 3D TAA kinematics *in vivo*, without being limited by skin movement artifacts and isolated from subtalar motion. Since the available amount of dorsiflexion is the crucial factor to allow unrestricted gait, walking uphill is an appropriate motion task to challenge and evaluate the performance of the TAA. **Clinical Relevance:** The presented method has the potential to identify specific kinematic patterns and thereby help clinicians and implant developers to evaluate current designs and future design modifications.

**Key Words:** Ankle Arthroplasty; Kinematics; Videofluoroscopy; Gait

### INTRODUCTION

The two most common methods of surgical treatment for ankle osteoarthritis are arthrodesis or total ankle arthroplasty (TAA). Arthrodesis has been associated with persistent alterations in gait due to a loss of ankle motion compensated with an increased motion of the neighboring small joints.<sup>14,15,44</sup> The long-term effect is a higher risk of osteoarthritis in those joints.<sup>6,28</sup> Replacement of the ankle joint gives the theoretical benefit of preservation of movement. An important design criterion of a TAA is to replicate the kinematics of a healthy ankle, namely to restore motion and at the same time to allow surrounding soft tissues to maintain their role of guiding and limiting motion.<sup>19</sup> Considering a TAA with unconstrained design, it is still not clear if, in the absence of the ability of transmitting transverse forces and axial moments by the articulating surfaces, a close to normal gait pattern may be restored and compatibility to the anatomical role of the surrounding soft tissues may be assured.<sup>10,21</sup> The knowledge of the *in vivo* performance of the TAA, especially including the kinematics during daily activities, is of high importance for the evaluation of the functionality of a TAA design.

Previous investigations on the kinematics of TAA include static radiographic measurements,<sup>7,33,45</sup> cadaver tests,<sup>27,32,36–39</sup> and gait analysis using skin markers.<sup>4,11,12,29,30,40</sup> Lateral two-dimensionally assessed static radiographic measurements are prone to projection errors

<sup>1</sup>Institute for Biomechanics, ETH Zurich, Switzerland.

<sup>2</sup>Foot and Ankle Center, Schulthess Clinic, Switzerland.

One or more of the authors has received or will receive benefits for personal or professional use from a commercial party related directly or indirectly to the subject of this article. In addition, benefits have been directed to an ISB student dissertation grant.

Corresponding Author:  
Renate List, PhD  
Institute for Biomechanics  
HCI E451 ETH Zurich  
8093 Zurich  
Switzerland  
Phone: +41 44 633 6764  
Fax: +41 44 633 1124  
rlist@ethz.ch

For information on pricings and availability of reprints, email reprints@datatrace.com or call 410-494-4994, x232.

induced by the positioning of the patient relative to the X-ray beam axis and cannot necessarily predict the dynamic behavior of the TAA. Cadaver excursion tests allow dynamic testing scenarios, but are limited by a lack of muscle activity and adaptive processes. Skin marker analyses allow the *in vivo* quantification of the gait characteristics. However, skin marker tracking has the drawback of skin movement artifacts, which is believed to be the most important error in human movement analysis.<sup>20</sup> A further limitation is the inaccessibility of the talus for attaching markers, thus the impossibility to distinguish tibiotalar from subtalar motion. Valuable findings concerning the kinematics of healthy ankle joints have been gained by bone pin measurements<sup>1,25,35</sup> and roentgen stereophotogrammetry using implanted tantalum markers.<sup>24</sup> However, the latter two measurement techniques are very unlikely to be applicable for the use on TAA patients due to their high invasiveness.

Single plane videofluoroscopic analysis<sup>3,17,46</sup> as well as dual orthogonal fluoroscopy<sup>23</sup> has provided valuable information regarding total knee arthroplasties. In the field of ankle and foot kinematics, 3D videofluoroscopic analyses of daily motion tasks were only rarely used up to now. By means of a combined magnetic resonance and dual-orthogonal fluoroscopic approach, the healthy ankle joint was investigated during a simulated stance phase with pausing at heel strike, midstance and toe off.<sup>9,42</sup> Komistek et al.<sup>18</sup> looked at the Buechel-Pappas TAA at three weightbearing positions when moving from maximum dorsi- to plantarflexion. Conti et al.<sup>8</sup> analyzed Agility patients and Leszko et al.<sup>22</sup> analyzed Salto patients in four positions of the stance phase of gait and a step-up motion. In summary, previous studies using an *in vivo* single plane videofluoroscopic approach, successfully determined the relative motion between the ankle implant components under dynamic conditions, but were limited to a small number of analyzed frames and/or restricted measurement set up, that did not allow the measurement of free gait.

To evaluate the functionality of a TAA design, the knowledge of the accurate 3D *in vivo* kinematics of its components is crucial and the kinematic measurement should fulfill the following requirements: analysis of the TAA motion *in vivo*, three-dimensionally, during daily motion tasks, such as free gait. Since arthrodesis patients particularly show limitations when walking uphill,<sup>26</sup> one should also include more challenging motion tasks for the ankle, such as slope walking. The sampling frequency should be reasonable to capture TAA motion during the stance phase of about 600 ms. The measurement should allow direct tracking of tibiotalar motion, isolated from subtalar motion and be free of skin movement artifacts.

Based on the above mentioned requirements, the aim of the present preliminary study was to quantify the 3D kinematics of the implant components of an unconstrained TAA with good outcomes during the stance phase of level, uphill, downhill and cross-slope walking using videofluoroscopy.

## MATERIALS AND METHODS

### Data acquisition

The experimental set up allowed the assessment of level gait, walking uphill, downhill and cross-slope walking. It consisted of a videofluoroscopy system integrated into a walkway 10 m in length and 1 m in width, with the height of the walking level 50 cm above the floor (Figure 1). The C-arm was inclined, with the X-ray source lower than the image intensifier, such that the bottom ray was parallel to the floor, resulting in a minimized shade of the floor and maximized usable field of view. A ramp with an inclination angle of 10 degrees and an accordingly adapted inclination and height of the C-arm were used for slope walking. The videofluoroscopic image capture was performed using the videofluoroscopy system BV Pulsera (Philips Medical Systems, Switzerland) with a field of view of 30.5 cm. The system modification allowed measurements to take place with a pulsed mode of 25 Hz, 8 ms radiation, 1 ms shutter time and a image resolution of 1000 x 1000 pixels with a grayscale resolution of 12 bit.<sup>13</sup> The fluoroscopy coordinate system was defined as follows: x- and y-axes lie in the image plane; z-axis was directed perpendicular to the image plane (Figure 1).

The test procedure consisted of the three main parts, calibration procedure, static trials and dynamic trials. The calibration procedure included one image of a well-defined calibration grid, used for image distortion correction and five images of a calibration tube, to estimate projection parameters of the fluoroscopic system. The subject had to perform six static trials: two standing trials in an anatomical upright position once captured from the side, once from the front, as well as a maximal plantarflexed, a maximal dorsiflexed, a maximal everted and a maximal inverted static loaded position. Each of the maximal deflected positions was repeated twice and the maximal of the two was selected. The dynamic trials included the assessment of the ankle kinematics during five gait conditions. Namely, level gait (gt), walking downhill (dnh), walking uphill (uph), and cross-slope walking, once sloping to the medial side (csm), and once to the lateral side (csl) of the ankle. For each of the five gait conditions the subjects had to perform five valid trials (stance phase

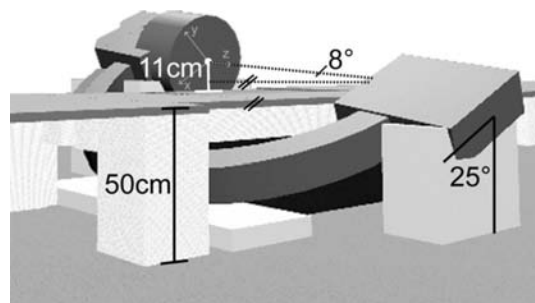


**Fig. 1:** Videofluoroscopy system integrated into walkway, set up for level gait.



**Fig. 2:** Three-dimensional reconstructed videofluoroscopic image.

captured). The mean and standard deviation of the five trials were calculated.

**Data processing**

Image distortion of the videofluoroscopic images was eliminated by a local correction algorithm using a reference grid with approximately 1,300 beads.<sup>13</sup> The projection parameters of the videofluoroscopic system (focal distance, location of the principle point in the image plane) were determined by a least-squares optimization using the images of the calibration tube.<sup>13</sup>

The 3D reconstruction of the 2D images was performed using the CAD models of the implant components and a registration algorithm, initially designed for the location of hip implants in X-ray images.<sup>5</sup> The respective output of the registration algorithm is the 3D position of the tibial and talar components (Figure 2). For the analysis of the error of the 2D/3D reconstruction, the tibial and the talar component of the Mobility™ Total Ankle, both of size three, were fixed together and embedded into polyurethane foam. Using a positioning set up, composed of a cross table and a marking

unit, the TAA components were captured in 63 positions.<sup>13</sup> Each image was 3D reconstructed using the CAD data of the manufacturer, and the translational as well as the rotational error were estimated for both components by means of the standard deviation (SD) of the 63 measurements. The rotational error was found to be smaller than 0.2 degrees in plane and 1.3 degrees out of plane. The translational error was smaller than 0.4 mm in plane and 2.1 mm out of plane.

Joint rotations and translations were described from the talar relative to the tibial component using a helical axis approach.<sup>43</sup> In other words, rotation angle and screw vector were extracted from the rotation matrix using quaternion calculations. To define clinically interpretable rotational components, the attitude vector (rotation angle multiplied with the normalized screw vector) was decomposed along the axes of the implant coordinate system, defined in the respective CAD data of the components (Figure 3). Neutral, thus 0 degrees, was defined by the initial position of the implant components determined by the implant coordinate system. TAA motion was furthermore analyzed by the location and orientation of the talar construction axis, defined by the cylinder axis of the talar component, relative to the tibial component (Figure 3).

Outcome parameters were defined for the static and the dynamic trials and are listed in Table 1. The definition of ROM for ankle dorsi-/plantarflexion is shown in Figure 4.

**Preliminary feasibility study**

Four male, good outcome patients, having had an unconstrained TAA on one side (Mobility™ Total Ankle, DePuy) participated in this study (Table 2). Inclusion criteria for the subjects included to be at least one year post-operative at time of testing, having a minimal American Orthopaedic Foot and Ankle Society ankle hindfoot score (AOFAS) of 90 points and a maximum of 1 point on a visual analog pain scale (VAS), clinically assessed in the year of testing. All four subjects had a well-aligned TAA, ensured by a post-operative clinically assessed anteroposterior radiograph. Each subject signed an informed consent form in accordance to the research ethics committee of the ETH Zurich.

The whole measurement procedure including 25 gait trials and 10 single pictures equated to a radiation exposure dose of

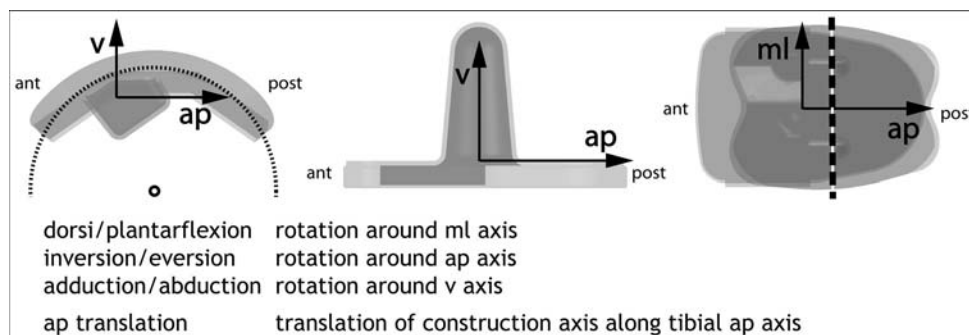


**Fig. 3:** Implant coordinate system (black arrows) – mediolateral (ml) axis, anteroposterior (AP) axis, vertical (v) axis and talar construction axis (black and white dashed line).

**Table 1:** Outcome Parameters**Static Clinical Rotation Parameters**

$max_{stat}pf$	sagittal plane orientation of the implant components in a maximal plantarflexed static loaded position
$max_{stat}df$	sagittal plane orientation of the implant components in a maximal dorsiflexed static loaded position
$ROM_{stat}pfd$	maximal ROM around the ml-axis between $max_{stat}pf$ and $max_{stat}df$
<i>StandingTrial</i>	sagittal plane orientation of the implant components in the upright standing trial
$ROM_{stat}invev$	ROM around the ap-axis between a maximal everted and a maximal inverted static loaded position

**Dynamic Clinical Rotation Parameters**

$max_{dyn}pf$	first peak of plantarflexion (see Figure 4)
$max_{dyn}df$	peak of dorsiflexion (see Figure 4)
$ROM_{dyn}pf$	ROM between heel strike and $max_{dyn}pf$ (see Figure 4)
$ROM_{dyn}df$	ROM between $max_{dyn}pf$ and $max_{dyn}df$ (see Figure 4)
$ROM_{dyn}pfd$	range between maximum and minimum of dorsi-/plantarflexion during stance
$ROM_{dyn}adab$	range between maximum and minimum of adduction/abduction during stance
$ROM_{dyn}invev$	range between maximum and minimum of inversion/eversion during stance
$ROM_{dyn}tap$	range between maximum and minimum of the anteroposterior translation during stance

ROM, range of motion.

approximately 0.05 mSv. This is equivalent to approximately 2.5 times the effective dose reported for a chest X-ray<sup>31</sup> and 200 times smaller than the effective dose reported for a CT scan of the abdomen or the pelvis.<sup>41</sup> Thus, the radiation exposure was minimal.

**RESULTS**

Results for the static clinical rotations of the four TAA subjects are given in Table 3. In the upright standing trials, all the TAA subjects showed, relative to the neutral position

of the implant components, a plantarflexed position of the talar relative to the tibial component (Table 3). Starting from the ankle in position of the standing trial, sub1, sub2 and sub3 showed at least 9 degrees of functional available range of motion (ROM) in the direction of dorsiflexion, whereas sub4 was limited to 1 degree. In the direction of plantarflexion, all subjects showed more than 10 degrees of functional available ROM compared to the upright standing trial position.

The TAA kinematics of level gait are presented in Figure 5, and sagittal plane kinematics of the four ramp conditions are

**Table 2:** Information on TAA Subjects

	sub1	sub2	sub3	sub4
Age [Years]	60	53	60	60
Height [m]	1.7	1.85	1.84	1.82
Weight [kg]	72	91	88	74
Years post-op	4.8	4.4	1.3	3.3
Pre-op Diagnoses	Primary OA	Primary OA	Primary OA rearfoot varus	Posttraumatic OA
Surgical Approach	anterior	anterior	anterior	anterior
Concomitant Procedures	release of the gastrocnemius aponeurosis	-	Dwyer osteotomy, deltoid release to rebalance the ankle	-
VAS	0	0	0	1
AOFAS	100	94	90	100

VAS and AOFAS were clinically assessed in the year of testing. OA, osteoarthritis; VAS, visual analog scale; AOFAS, American Orthopaedic Foot and Ankle Society ankle hindfoot score.

**Table 3:** Static Clinical Rotations Parameters of Each Subject and Mean and SD Over All Subjects

Static Trials [degrees]	Rotation around ml-axis				Rotation around ap-axis
	$max_{stat}df$	$max_{stat}pf$	$ROM_{stat}pfd$	Standing Trial	$ROM_{stat}invev$
sub1	1.9	-19.3	21.2	-7.1	0.8
sub2	3.5	-38.2	41.7	-11.4	3.5
sub3	5.6	-25.0	30.6	-9.0	2.1
sub4	-6.6	-20.9	14.3	-7.8	4.3
mean ± SD	1.1 ± 5.4	-25.9 ± 8.6	27.0 ± 11.9	-8.8 ± 1.9	2.7 ± 1.5

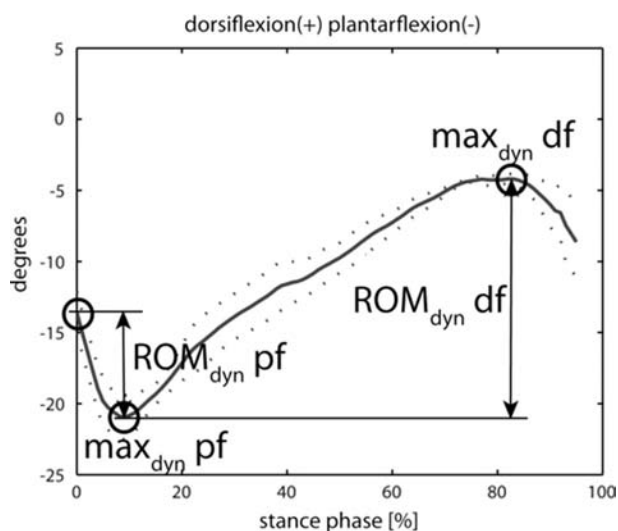


**Fig. 4:** Definition of ROM for ankle dorsi-/plantarflexion.

shown in Figure 6. Results of the dynamic clinical rotation parameters are given in Table 4 for the sagittal plane and in Table 5 for the frontal and the transverse plane rotations, as well as for anteroposterior translation. The predominant motion at the TAA for all gait tasks was dorsi-/plantarflexion. The motion pattern showed, for all four TAA subjects, the following characteristics: after heel strike the TAA experienced a plantarflexion motion, followed by dorsiflexion and another shift in the plantarflexion direction. Concerning the timing, the minimum for all subjects was around 10% of stance, whereas sub1, sub2 and sub4 reached the maximum

between 70% to 90% of stance, but sub3 already reached it around 40% (Figure 6). The inter-individual differences for sagittal plane motion were large showing values between 0.3 and 10.4 degrees, and 2.8 and 17.1 degrees for  $ROM_{dyn}pf$  and  $ROM_{dyn}df$ , respectively (Table 4).

The TAA experienced only minimal inversion/eversion and adduction/abduction motion (Table 5). Their rotation amplitudes were in the range of the variability (Figure 5 an ex-ample for level gait). A characteristic motion pattern was not recognizable for either of them. The talar construction axis showed less than 4.6 mm of translation along the AP axis and stayed more or less parallel for all subjects and all conditions (Figure 7).

When comparing walking uphill to level gait, all subjects showed less  $ROM_{dyn}pf$ , as well as less  $ROM_{dyn}df$  (Table 4). Walking downhill showed the tendency of an increase in  $ROM_{dyn}pf$  compared to level gait. A systematic change in ROM was not present for cross-slope walking.

**DISCUSSION**

The developed procedure enabled quantification of TAA kinematics, without being limited by skin movement artifacts. Hereby motion at the TAA is isolated from motion of the subtalar joint. The experimental set up allowed the TAA subjects to walk freely on level ground, as well as on ramps with an inclination of 10 degrees.

Although the present study is limited by its small patient sample and the impossibility of drawing a general conclusion concerning TAA outcome, the present data confirmed the

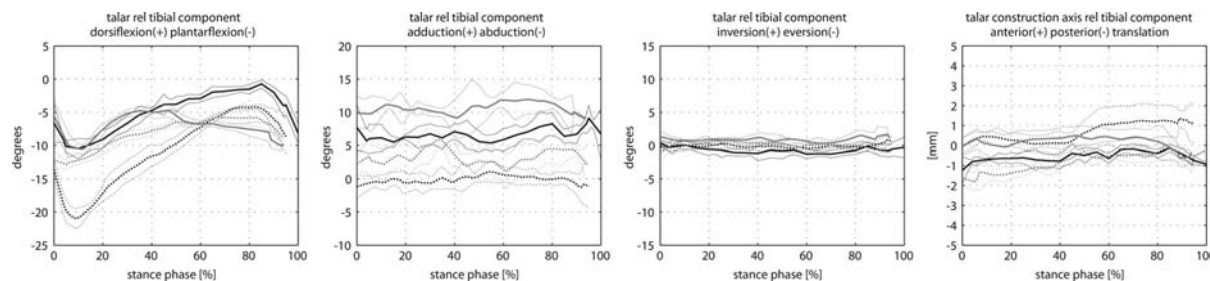


**Fig. 5:** Ankle kinematics during the stance phase of level gait. Mean and SD of all trials for each subject: sub1 (black solid line), sub2 (black dotted line), sub3 (gray solid line), sub4 (gray dotted line).

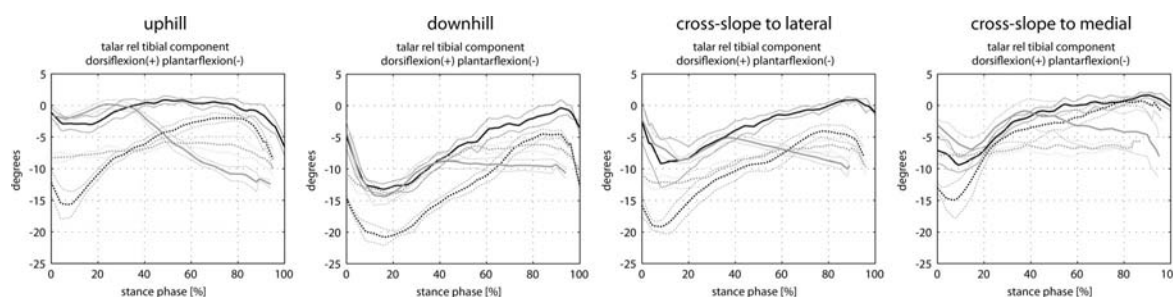


**Fig. 6:** Ankle sagittal plane kinematics during the stance phase of slope walking (from left to right): uphill, downhill, cross-slope to lateral, cross-slope to medial. Mean and SD of all trials for each subject: sub1 (black solid line), sub2 (black dotted line), sub3 (gray solid line), sub4 (gray dotted line).

need to investigate dynamic daily activities, such as gait, following TAA. It is not only the magnitude of static available ROM which determines if the TAA restricts gait, but, most important, how it is situated functionally and how effectively it can be used, so that daily motion tasks may be performed without inducing compensation movements in adjacent joints.

The static trials revealed that the TAA allows marginal motion in the frontal plane and large inter-individual differences in the sagittal plane. Even so all four subjects showed values for sagittal plane maximal static ROM that were comparable to radiographically assessed tibiotalar ROM of the Agility TAA<sup>7</sup> and of the STAR Ankle<sup>TM</sup> prosthesis,<sup>45</sup> as well as to the fluoroscopy gained ROM of the Buechel-Pappas TAA.<sup>18</sup> Three of the four subjects showed a rather diminished sagittal ROM in comparison to the tibiotalar ROM of healthy ankles analyzed in previous studies.<sup>2,9,18,24,34</sup> Starting from the upright standing trial position, the TAA subjects showed a smaller functionally available dorsiflexion ROM, than plantarflexion. This one-sided restriction in dorsiflexion has also been observed in previous skin marker studies,<sup>11,29</sup> as well as in cadaver studies.<sup>32,37</sup> Since the polyethylene inlay and the talar component both show a double curved shape, it can be assumed that during the small amount of frontal plane motion the congruency can more or less be maintained and no increased risk of wear should arise.

During level gait only minor limitations in sagittal plane motion were found for the TAA subjects. Restrictions were mainly seen during walking uphill due to a dorsiflexion limitation. It can be assumed that the TAA allows maintenance of motion and preserves adjacent joints from compensatory movements. A further improvement of the functionality of the TAA could possibly be achieved by balancing the static available to the functional ROM needed during gait by a change in implant positioning during surgery or by intensified physiotherapy.

For all gait conditions, dorsi-/plantarflexion was the predominant rotation occurring at the TAA. The sagittal plane motion pattern observed during level gait, with a plantarflexion peak at around 10% and a dorsiflexion peak at around 80% of stance, is comparable to the kinematics of

healthy ankles in the bone pin studies by Arndt et al.<sup>1</sup> and Lundgren et al.<sup>25</sup> Only sub3 reached the dorsiflexion peak before midstance and therefore showed atypical behavior with regard to timing. In contrast, Leszko et al.<sup>22</sup> reported an almost linear motion pattern for dorsi-/plantarflexion during level gait and a step up task for the Salto TAA. However, since in the study of Leszko et al.<sup>22</sup> only four images (heel strike, 33% stance, 66% stance, toe off) were analyzed, it can be assumed that imperative information was lacking due to the insufficient sampling frequency. Nevertheless the mean sagittal ROM during level gait is in agreement with the study of Leszko et al.<sup>22</sup> Compared to gait data of healthy ankles in studies by Lundgren et al.<sup>25</sup> and Arndt et al.<sup>1</sup> sagittal ROM of the TAA subjects showed only minor reductions during gait.

Inversion/eversion, as well as adduction/abduction, during gait was small but showed large variability, which has also been stated by Conti et al.<sup>8</sup> Compared to the characteristic frontal<sup>1,25</sup> and transverse<sup>1</sup> plane kinematics described for healthy ankles, the TAA subjects did not replicate transverse and frontal plane motion characteristics of a healthy ankle, even though the maximal ROM was similar. Neither the frontal plane motion characteristics of the healthy ankle, described as an initial inversion up to 20% stance, followed by eversion, followed by more or less a static behavior and a final strong inversion during the last 10% stance,<sup>1,25</sup> nor the transverse plane motion characteristics of an adduction movement that followed an initial abduction movement during the first 20% stance,<sup>1</sup> was seen for the TAA (Figure 5). In the unconstrained TAA the articulating surfaces account for less constraint than in a healthy ankle. Nonetheless, it remains unclear, whether the inability to transmit transverse forces and axial moments by the articulating surfaces or whether the influence of the changed geometric arrangements of the surrounding soft tissues, e.g., as lever arms of ligaments, tendons and muscles was the main reason for not restoring frontal and transverse plane motion patterns of healthy ankles. However, since the outcome of a TAA is dependent on the compatibility between the TAA and the surrounding ligaments,<sup>19</sup> the influence of the changed motion pattern of such an unconstrained TAA on the surrounding soft tissues should be addressed in future studies.

**Table 4:** Dynamic clinical rotation parameters  $ROM_{dyn} pf$  and  $ROM_{dyn} df$

$ROM_{dyn}$ [degrees]	gt		uph		dnh		csl		esm	
	pf	df	pf	df	pf	df	pf	df	pf	df
sub 1	3.9 ± 2.8	10.3 ± 1.4	2.5 ± 1.3	5.0 ± 0.8	8.7 ± 2.3	13.3 ± 1.7	7.8 ± 3.8	11.0 ± 3.1	2.4 ± 1.9	11.4 ± 1.6
sub 2	7.5 ± 1.7	17.1 ± 1.7	3.9 ± 1.6	14.3 ± 2.4	6.3 ± 1.4	16.7 ± 1.7	3.7 ± 2.6	15.6 ± 1.2	2.5 ± 2.6	16.8 ± 2.8
sub 3	5.6 ± 2.4	6.5 ± 1.4	0.9 ± 1.2	2.8 ± 0.9	10.4 ± 2.3	6.0 ± 1.1	6.7 ± 2.6	3.9 ± 0.6	4.0 ± 1.5	6.5 ± 2.7
sub 4	0.9 ± 1.4	7.7 ± 1.1	0.3 ± 0.4	3.3 ± 0.8	3.5 ± 0.9	8.7 ± 1.1	1.8 ± 0.9	6.9 ± 0.8	0.4 ± 0.3	2.8 ± 0.9
mean ± SD	4.5 ± 2.8	10.4 ± 4.7	1.9 ± 1.6	6.3 ± 5.4	7.2 ± 3.0	11.2 ± 4.8	5.0 ± 2.8	9.3 ± 5.1	2.3 ± 1.5	9.4 ± 6.1

Mean and SD of all trials of each subject during the stance phase of all five gait tasks. Last row: mean and SD over all four subjects.

**Table 5:** Dynamic clinical rotation parameters  $ROM_{dyn} adab$ ,  $ROM_{dyn} invev$ , and  $ROM_{dyn} t_{ap}$

$ROM_{dyn}$	gt		uph		dnh		csl		esm	
	$adab$ [degrees]	$t_{ap}$ [mm]	$adab$ [degrees]	$t_{ap}$ [mm]	$adab$ [degrees]	$t_{ap}$ [mm]	$adab$ [degrees]	$t_{ap}$ [mm]	$adab$ [degrees]	$t_{ap}$ [mm]
sub 1	7.2 ± 1.8	3.1 ± 0.5	2.7 ± 0.6	1.7 ± 0.4	2.5 ± 0.2	3.4 ± 0.6	8.8 ± 4.7	2.8 ± 0.2	2.7 ± 0.8	5.1 ± 0.8
sub 2	4.4 ± 1.0	2.0 ± 0.4	3.0 ± 0.8	2.8 ± 0.9	2.7 ± 1.1	4.4 ± 1.0	12.6 ± 4.8	2.9 ± 0.7	3.4 ± 0.7	5.0 ± 0.9
sub 3	6.6 ± 0.9	2.2 ± 0.4	1.9 ± 0.6	2.6 ± 0.3	2.5 ± 0.5	2.8 ± 0.3	9.3 ± 2.3	2.3 ± 0.8	1.8 ± 0.3	6.0 ± 1.4
sub 4	7.8 ± 1.6	3.1 ± 0.5	1.2 ± 0.2	2.9 ± 0.8	3.4 ± 0.9	1.7 ± 0.2	14.0 ± 3.6	3.2 ± 0.6	1.7 ± 0.3	7.5 ± 0.5
mean ± SD	6.5 ± 1.5	2.6 ± 0.6	2.4 ± 1.2	2.6 ± 0.5	2.8 ± 0.4	3.1 ± 1.1	11.2 ± 2.5	2.8 ± 0.4	2.4 ± 0.8	5.9 ± 1.1

Mean and SD of all trials of each subject during the stance phase of all five gait tasks. Last row: mean and SD over all four subjects.

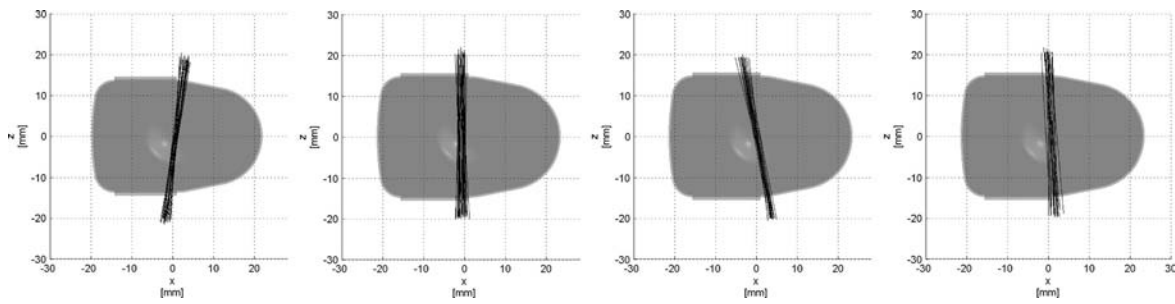


**Fig. 7:** Motion of the talar construction axis relative to the tibial component during one typical level gait trial of each subject. From left to right: sub1, sub2, sub3, sub4.

The shifts in adduction/abduction present between subjects (Figure 5) show the differences in transverse rotation, which are dependent on the alignment between the TAA components set during surgery. This transverse plane misalignment was also seen in the standing trials and the orientation of the talar construction axes during level gait (Figure 7).

Even though the analyzed TAA is an unconstrained design, which allowed free translation in the transverse plane, the measured anteroposterior translation of the cylinder axis relative to the tibial component was small in agreement with the findings of Conti et al.<sup>8</sup> and Leszko et al.<sup>22</sup> Furthermore, since the construction axis stayed more or less parallel and only showed little translation, it can be concluded that the main rotation occurred around the construction axis itself. Since this motion path is according to the motion path dictated by the geometry of the TAA, it permits to maintain an optimal congruency of the implant components which leads to a better load distribution along the articulating surfaces and is therefore favorable for the wear characteristics of the TAA. Whether such a motion path will allow a physiological role of the surrounding ligaments remains to be seen.

For optimal function, the static available ROM needs to be distributed over a range that fully enables the performance of dynamic gait tasks without restrictions. A comparison between the static available ROM ( $ROM_{stat}pfd$ ) and the ROM which was actually used during the dynamic motion tasks ( $ROM_{dyn}pfd$ ), is graphically provided in Figure 8.

Generally, the static available ROM was shifted compared to the ROM that was functionally used during gait (asymmetric vertical bar pattern). Therefore, in terms of distribution of the unexploited motion ranges, an asymmetry with a larger range of plantarflexion than of dorsiflexion was seen ( $\Delta pf > \Delta df$ ). Based on this shift, it can be concluded that the static available ROM cannot be used effectively, since it is not distributed functionally in terms of the requirements for gait. A possible restriction during gait, due to a limitation in the static available ROM was seen for sub4 during all gait tasks and for sub1 during uphill and cross-slope walking ( $\Delta df$  missing or marginal). All restrictions concerned the direction of dorsiflexion. On the contrary, the available range of plantarflexion was not even closely exploited for any of the subjects and any of the gait conditions.

Even though the design of the Mobility™ Total Ankle allows the same amount of motion in both directions, decreased ROM in dorsiflexion was found. The restriction in dorsiflexion is in line with the findings of a cadaver study of Richter et al.<sup>32</sup> which investigated the Hintegra TAA, whereas the same study found no differences for the German Ankle System. Thus, based on the latter study the design may have an influence. Coetzee and Castro<sup>7</sup> stated in their study on 61 patients who had a primary Agility TAA, that the main factor determining the postoperative ROM is the preoperative ROM. Whether this finding can be applied to other designs is unclear. However, on the basis of the latter study, the restrictions could also be due to other factors than the design of the

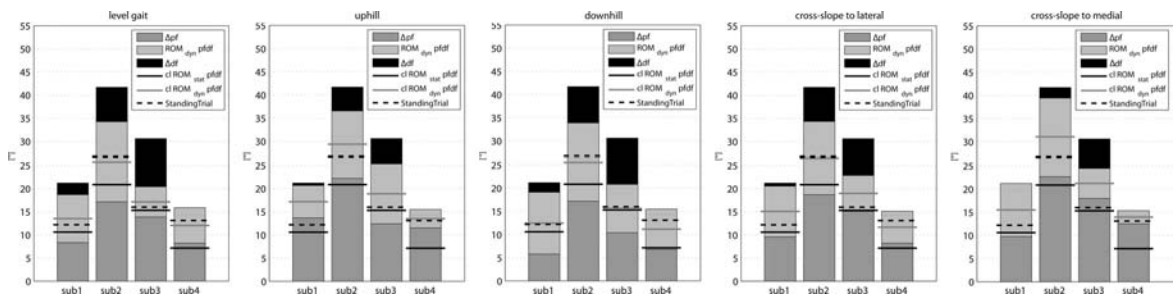


**Fig. 8:** Sagittal plane static versus dynamic ROM. Whole bar (black + dark gray + light gray) refers to  $ROM_{stat}pfd$ . The light gray part shows the functional ROM used during gait ( $ROM_{dyn}pfd$ ). The black and the dark gray parts show the unexploited motion ranges in the direction of dorsiflexion  $\Delta df$  (black) and plantarflexion  $\Delta pf$  (dark gray), and give a measure of how much of  $ROM_{stat}pfd$  was used during the dynamic gait tasks. The dotted line gives the reference of the orientation of the components in the upright standing trial. The centerlines,  $cl ROM_{stat}pfd$  and  $cl ROM_{dyn}pfd$ , allow an estimate of how well situated the range of available motion is.



prosthesis alone. Hintermann et al.<sup>16</sup> found the main reason of the restriction to be the scarred capsule and soft tissues. Doets et al.<sup>11</sup> and similarly Benedetti et al.<sup>4</sup> concluded that there was more co-contraction in TAA subjects than in controls. For that reason, the decreased sagittal ROM could be explained by the restraints of the surrounding muscular co-contraction. Future studies need to address whether the main causes for the restriction in ROM in pain-free subjects are stiffness of the surrounding soft tissues, changed muscular activity, implant design or of multifactorial nature. Furthermore, it should be clarified if these restrictions and their causes are implant design specific or may be generalized.

Depending on the foot size, the TAA left the field of view of the image intensifier before toe off. This limitation only allowed the whole stance phase to be tracked for sub1. However, the second half of the stance phase was of less interest, since the healthy talocrural joint demonstrates more motion during the first half than during the second half of the stance phase.<sup>9</sup> An additional limitation is the out of plane accuracy given by the single plane approach. However, the present accuracy of the 2D/3D reconstruction is in the range of, or even better than, the 2D/3D reconstruction algorithms presented by referenced past studies on single plane videofluoroscopy with knee prosthesis.<sup>3,17</sup>

## CONCLUSION

The presented videofluoroscopic procedure enabled accurate estimation of the 3D TAA kinematics *in vivo*, without being limited by skin movement artifacts and it was isolated from subtalar motion. This preliminary feasibility study showed the applicability of the procedure and confirmed the importance of *in vivo* analysis of tibiotalar motion during daily activities. In comparison to previous bone pin studies on healthy ankles,<sup>1,25</sup> sagittal plane motion characteristics of the four TAA subjects with good outcomes were in line with healthy ankles, whereas transverse and frontal plane motion characteristics of healthy ankles were not replicated by the TAA subjects. It remains to be seen if those small differences (less than 5 degrees) have a relevant impact on the strain behavior of the surrounding soft tissues. Contrary to expectations, cross-slope walking did not provoke any instability in the behavior of the TAA. It was found that the available amount of dorsiflexion was the crucial factor to allow unrestrictive gait, whereas the available amount of plantarflexion seemed to be sufficient for any of the analyzed gait tasks. The current study showed that walking uphill was an appropriate motion task to challenge and evaluate the performance of the TAA with good outcomes. The developed procedure has the potential to help clinicians and implant developers to evaluate current designs and future design modifications, if it is applied to a larger number of subjects.

## ACKNOWLEDGEMENTS

In memory of Dr. Alex Stacoff †: an amazing mentor, advisor, and friend.

## REFERENCES

1. **Arndt, A; Westblad, P; Winson, I; Hashimoto, T; Lundberg, A:** Ankle and subtalar kinematics measured with intracortical pins during the stance phase of walking. *Foot Ankle Int.* **25:** 357-364, 2004.
2. **Backer, M; Kofoed, H:** Passive ankle mobility. Clinical measurement compared with radiography. *J Bone Joint Surg Br.* **71:** 696-698, 1989.
3. **Banks, SA; Hodge, WA:** Accurate measurement of three-dimensional knee replacement kinematics using single-plane fluoroscopy. *IEEE Trans Biomed Eng.* **43:** 638-649, 1996. <http://dx.doi.org/10.1109/10.495283>
4. **Benedetti, MG; Leardini, A; Romagnoli, M; et al.:** Functional outcome of meniscal-bearing total ankle replacement: a gait analysis study. *J Am Podiatr Med Assoc.* **98:** 19-26, 2008.
5. **Burckhardt, K; Szekely, G; Notzli, H; Hodler, J; Gerber, C:** Submillimeter measurement of cup migration in clinical standard radiographs. *IEEE Trans Med Imaging.* **24:** 676-688, 2005. doi:10.1109/TMI.2005.846849 <http://dx.doi.org/10.1109/TMI.2005.846849>
6. **Coester, LM; Saltzman, CL; Leupold, J; Pontarelli, W:** Long-term results following ankle arthrodesis for post-traumatic arthritis. *J Bone Joint Surg Am.* **83-A:** 219-228, 2001.
7. **Coetzee, JC; Castro, MD:** Accurate measurement of ankle range of motion after total ankle arthroplasty. *Clin Orthop Relat Res.* 27-31, 2004. <http://dx.doi.org/10.1097/01.blo.0000132180.69464.84>
8. **Conti, S; Lalonde, KA; Martin, R:** Kinematic analysis of the agility total ankle during gait. *Foot Ankle Int.* **27:** 980-984, 2006.
9. **De Asla, RJ; Wan, L; Rubash, HE; Li, G:** Six DOF in vivo kinematics of the ankle joint complex: Application of a combined dual-orthogonal fluoroscopic and magnetic resonance imaging technique. *J Orthop Res.* **24:** 1019-1027, 2006. <http://dx.doi.org/10.1002/jor.20142>
10. **Detwyler, M; Stacoff, A; Kramers de Quervain, IA; Stuessi, E:** Modelling of the ankle joint complex. Reflections with regards to ankle prostheses. *Foot and ankle Surgery.* **10:** 109-119, 2004. <http://dx.doi.org/10.1016/j.fas.2004.06.003>
11. **Doets, HC; van Middelkoop, M; Houdijk, H; Nelissen, RG; Veeger, HE:** Gait analysis after successful mobile bearing total ankle replacement. *Foot Ankle Int.* **28:** 313-322, 2007. <http://dx.doi.org/10.3113/FAI.2007.0313>
12. **Dyrby, C; Chou, LB; Andriacchi, TP; Mann, RA:** Functional evaluation of the Scandinavian Total Ankle Replacement. *Foot Ankle Int.* **25:** 377-381, 2004.
13. **Foresti, M:** In vivo measurement of total knee joint replacement kinematics and kinetics during stair descent. *ETH Zurich, Zurich.* 2009. doi:10.3929/ethz-a-006036373 <http://dx.doi.org/10.3929/ethz-a-006036373>
14. **Gellmann, H; Lenihan, M; Halikis, N; et al.:** Selective tarsal arthrodesis: An in vitro analysis of the effect on foot. *American Orthopaedic Foot and Ankle Society.* **8:** 127-133, 1987.
15. **Hintermann, B; Nigg, BM:** Influence of arthrodeses on kinematics of the axially loaded ankle complex during dorsiflexion/plantarflexion. *Foot Ankle Int.* **16:** 633-636, 1995.
16. **Hintermann, B; Valderrabano, V; Dereymaeker, G; Dick, W:** The HINTEGRA ankle: rationale and short-term results of 122 consecutive ankles. *Clin Orthop Relat Res.* 57-68, 2004. <http://dx.doi.org/10.1097/01.blo.0000132462.72843.e8>
17. **Hoff, WA; Komistek, RD; Dennis, DA; Gabriel, SM; Walker, SA:** Three-dimensional determination of femoral-tibial contact positions under in vivo conditions using fluoroscopy. *Clin Biomech (Bristol,*

- Avon). **13**: 455-472, 1998. [http://dx.doi.org/10.1016/S0268-0033\(98\)00009-6](http://dx.doi.org/10.1016/S0268-0033(98)00009-6)
18. **Komistek, RD; Stiehl, JB; Buechel, FF; Northcut, EJ; Hajner, ME:** A determination of ankle kinematics using fluoroscopy. *Foot Ankle Int.* **21**: 343-350, 2000. PMID:10808976
  19. **Leardini, A:** Geometry and mechanics of the human ankle complex and ankle prosthesis design. *Clinical Biomechanics.* **16**: 706-709, 2001. [http://dx.doi.org/10.1016/S0268-0033\(01\)00022-5](http://dx.doi.org/10.1016/S0268-0033(01)00022-5)
  20. **Leardini, A; Chiari, L; Della Croce, U; Cappozzo, A:** Human movement analysis using stereophotogrammetry. Part 3. Soft tissue artifact assessment and compensation. *Gait Posture.* **21**: 212-225, 2005. <http://dx.doi.org/10.1016/j.gaitpost.2004.05.002>
  21. **Leardini, A; Moschella, D:** Dynamic simulation of the natural and replaced human ankle joint. *Med Biol Eng Comput.* **40**: 193-199, 2002. <http://dx.doi.org/10.1007/BF02348124>
  22. **Leszko, F; Komistek, RD; Mohfouz, MR; et al.:** In vivo determination of the mobile bearing total ankle prosthesis kinematics. In 54th Annual Meeting of the Orthopaedic Research Society, San Francisco, California, 2008.
  23. **Li, G; Wuerz, TH; DeFrate, LE:** Feasibility of using orthogonal fluoroscopic images to measure in vivo joint kinematics. *J Biomech Eng.* **126**: 314-318, 2004. <http://dx.doi.org/10.1115/1.1691448>
  24. **Lundberg, A; Goldie, I; Kalin, B; Selvik, G:** Kinematics of the Ankle Foot Complex - Plantarflexion and Dorsiflexion. *Foot and Ankle.* **9**: 194-200, 1989.
  25. **Lundgren, P; Nester, C; Liu, A, et al.:** Invasive in vivo measurement of rear-, mid- and forefoot motion during walking. *Gait Posture.* **28**: 93-100, 2008. <http://dx.doi.org/10.1016/j.gaitpost.2007.10.009>
  26. **Mazur, JM; Schwartz, E; Simon, SR:** Ankle arthrodesis. Long-term follow-up with gait analysis. *J Bone Joint Surg Am.* **61**: 964-975, 1979.
  27. **Michelson, JD; Schmidt, GR; Mizel, MS:** Kinematics of a total arthroplasty of the ankle: comparison to normal ankle motion. *Foot Ankle Int.* **21**: 278-284, 2000.
  28. **Muir, DC; Amendola, A; Saltzman, CL:** Long-term outcome of ankle arthrodesis. *Foot Ankle Clin.* **7**: 703-708, 2002. [http://dx.doi.org/10.1016/S1083-7515\(02\)00048-7](http://dx.doi.org/10.1016/S1083-7515(02)00048-7)
  29. **Muller, S; Wolf, S; Doderlein, L:** Three-dimensional analysis of the foot following implantation of a HINTEGRA ankle prosthesis: evaluation with the Heidelberg foot model. *Orthopade.* **35**: 506-512, 2006. <http://dx.doi.org/10.1007/s00132-006-0937-7>
  30. **Piriou, P; Culpán, P; Mullins, M; et al.:** Ankle replacement versus arthrodesis: a comparative gait analysis study. *Foot Ankle Int.* **29**: 3-9, 2008. doi:10.3113/FAI.2008.0003 <http://dx.doi.org/10.3113/FAI.2008.0003>
  31. **Quinn, AD; Taylor, CG; Sabharwal, T; Sikdar, T:** Radiation protection awareness in non-radiologists. *Br J Radiol.* **70**: 102-106, 1997.
  32. **Richter, M; Zech, S; Westphal, R; Klimesch, Y; Gosling, T:** Robotic cadaver testing of a new total ankle prosthesis model (German Ankle System). *Foot Ankle Int.* **28**: 1276-1286, 2007. <http://dx.doi.org/10.3113/FAI.2007.1276>
  33. **Rippstein, PF:** Clinical experiences with three different designs of ankle prostheses. *Foot Ankle Clin.* **7**: 817-831, 2002. [http://dx.doi.org/10.1016/S1083-7515\(02\)00058-X](http://dx.doi.org/10.1016/S1083-7515(02)00058-X)
  34. **Sammarco, GJ; Burstein, AH; Frankel, VH:** Biomechanics of the ankle: A kinematic study. *Orthop Clin North Am.* **4**: 75, 1973.
  35. **Stacoff, A; Nigg, BM; Reinschmidt, C; van den Bogert, AJ; Lundberg, A:** Tibiocalcaneal kinematics of barefoot versus shod running. *J Biomech.* **33**: 1387-1395, 2000. [http://dx.doi.org/10.1016/S0021-9290\(00\)00116-0](http://dx.doi.org/10.1016/S0021-9290(00)00116-0)
  36. **Tochigi, Y; Rudert, MJ; Brown, TD; McIlff, TE; Saltzman, CL:** The effect of accuracy of implantation on range of movement of the Scandinavian Total Ankle Replacement. *J Bone Joint Surg Br.* **87**: 736-740, 2005. <http://dx.doi.org/10.1302/0301-620X.87B5.14872>
  37. **Valderrabano, V; Hintermann, B; Nigg, BM; Stefanyshyn, D; Stergiou, P:** Kinematic changes after fusion and total replacement of the ankle: part 1: Range of motion. *Foot Ankle Int.* **24**: 881-887, 2003.
  38. **Valderrabano, V; Hintermann, B; Nigg, BM; Stefanyshyn, D; Stergiou, P:** Kinematic changes after fusion and total replacement of the ankle: part 2: Movement transfer. *Foot Ankle Int.* **24**: 888-896, 2003.
  39. **Valderrabano, V; Hintermann, B; Nigg, BM; Stefanyshyn, D; Stergiou, P:** Kinematic changes after fusion and total replacement of the ankle: part 3: Talar movement. *Foot Ankle Int.* **24**: 897-900, 2003.
  40. **Valderrabano, V; Nigg, BM; von Tscharnner, V; et al.:** Gait analysis in ankle osteoarthritis and total ankle replacement. *Clin Biomech (Bristol, Avon).* **22**: 894-904, 2007. <http://dx.doi.org/10.1016/j.clinbiomech.2007.05.003>
  41. **Wall, BF; Hart, D:** Revised radiation doses for typical X-ray examinations. Report on a recent review of doses to patients from medical X-ray examinations in the UK by NRPB. National Radiological Protection Board. *Br J Radiol.* **70**: 437-439, 1997.
  42. **Wan, L; de Asla, RJ; Rubash, HE; Li, G:** In vivo cartilage contact deformation of human ankle joints under full body weight. *J Orthop Res.* **26**: 1081-1089, 2008. <http://dx.doi.org/10.1002/jor.20593>
  43. **Woltring, HJ:** 3-D attitude representation of human joints: a standardization proposal. *Journal of Biomechanics.* **27**: 1399-1414., 1994. [http://dx.doi.org/10.1016/0021-9290\(94\)90191-0](http://dx.doi.org/10.1016/0021-9290(94)90191-0)
  44. **Wu, WL; Su, FC; Cheng, YM; et al.:** Gait analysis after ankle arthrodesis. *Gait Posture.* **11**: 54-61, 2000. [http://dx.doi.org/10.1016/S0966-6362\(99\)00049-1](http://dx.doi.org/10.1016/S0966-6362(99)00049-1)
  45. **Zerahn, B; Kofod, H:** Bone mineral density, gait analysis, and patient satisfaction, before and after ankle arthroplasty. *Foot Ankle Int.* **25**: 208-214, 2004.
  46. **Zihlmann, MS; Gerber, H; Stacoff, A; et al.:** Three-dimensional kinematics and kinetics of total knee arthroplasty during level walking using single plane video-fluoroscopy and force plates: a pilot study. *Gait Posture.* **24**: 475-481, 2006. <http://dx.doi.org/10.1016/j.gaitpost.2005.12.012>